This is a repository copy of *Modelling of H₂ production in a packed bed reactor via sorption enhanced steam methane reforming process*.

White Rose Research Online URL for this paper:
http://eprints.whiterose.ac.uk/117799/

Version: Accepted Version

Modelling of H₂ production in a packed bed reactor via sorption enhanced steam methane reforming process

S. Z. Abbas[*], V. Dupont, T. Mahmud

School of Chemical and Process Engineering, University of Leeds, LS2 9JT, UK

ABSTRACT

The sorption enhanced steam reforming (SE-SMR) of methane over the surface of 18 wt. % Ni/ Al_2O_3 catalyst and using CaO as a CO_2-sorbent is simulated for an adiabatic packed bed reactor. The developed model accounts for all the aspects of mass and energy transfer, in both gas and solid phase along the axial direction of the reactor. The process was studied under temperature and pressure conditions used in industrial SMR operations. The simulation results were compared with equilibrium calculations and modelling data from literature. A good agreement was obtained in terms of CH_4 conversion, hydrogen yield (wt. % of CH_4 feed), purity of H_2 and CO_2 capture under the different operation conditions such as temperature, pressure, steam to carbon ratio (S/C) and gas mass flux. A pressure of 30 bar, 923 K and S/C of 3 can result in CH_4 conversion and H_2 purity up to 65% and 85% respectively compared to 24% and 49% in the conventional process.

Keywords: Mathematical modelling; Sorption enhanced steam methane reforming; Simulation; Equilibrium

[*]Corresponding Author

Tel.: +44-7451919251
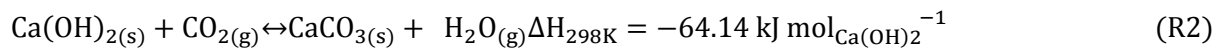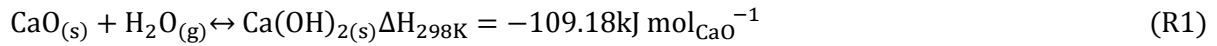
E-mail address: pmsza@leeds.ac.uk

1. Introduction

In any industrial chemical process, the reactor is considered as the heart of the process. In a catalytic reactor, reactions between the reactants take place on the surface of the catalyst. Downstream of the reactor, separation is required to achieve high product purity. Separation processes are usually very costly and contribute towards higher investment and operational costs [1]. Mayorga et al.[2] presented a concept of a reactor in which reaction and separation took place at the same time in a single reactor. This concept of hybrid reactor reduces the capital cost of the process, as no downstream unit operation is required to achieve the desired product purity.

CO_2 accounts for 99 wt.% of total greenhouse gas emission [3],causing global warming. Almost 75% of CO_2emission in the atmosphere for the last 20 years is due to the burning of the fossil fuels [4]. Fired processes in the chemical industry represent a significant contribution to total CO_2 emissions in developed countries. Due to increasing concern about the CO_2 emission, attention has been given to manage CO_2 emission during the conventional steam methane reforming (SMR) process. The SMR process is the most widely used technique for H_2 production and over 50% of the world's H_2 production is from the SMR process [4]. The higher degree of endothermicity of the process makes it operate at high temperature conditions. In industrial SMR processes, CO-shift reactors are needed downstream of the reformer to convert the undesired CO and steam into CO_2 and H_2 product. Later on, amine scrubbing or pressure swing adsorption (PSA) process is required to achieve the higher purity of H_2 [5]. To address the issue of global warming, researchers developed the concept of combining the reforming process with in-situ CO_2 separation by solid adsorption. This process was named sorption enhanced steam methane reforming (SE-SMR) process [5-7].

The SE-SMR is the process that produces H_2 and at the same time captures CO_2 by featuring a CO_2 sorbent in the reactor. This process works on the principle of hybrid reactor as presented by Mayorga et al. [2]. Williams et al. [5] issued a patent in which they explained the SE-SMR process for the production of H_2. Tsekhovoi et al. [6] showed that the SE-SMR process saves the overall energy demand of the system and this process has the potential of saving up to 20-25% energy as compared to the conventional SMR process. The SE-SMR process has the advantage of increasing CH_4 conversion, H_2 production and removing CO_2 from the product stream. As the CO_2 is captured on a sorbent, the equilibrium of water gas shift (WGS) reactions results in more H_2 production at low temperature (723-873 K) than the conventional SMR process (1073-1300 K) [7, 8]. In SE-SMR process, no WGS reactor is required downstream of the steam methane reformer unlike the conventional SMR process [9].

Fernández et al. [10] compared the performance of different sorbents on the basis of H_2 yield. They reported that using CaO as sorbent results in a weakly exothermic process, whilst using Li_2ZrO_3 makes the overall reaction weakly endothermic. In order to enhance the conversion of CH_4 and achieve a maximum net efficiency, S/C for each process was adjusted and optimum operating temperature and pressure was derived. It was concluded from the findings that CaO is the most favourable CO_2 sorbent from thermodynamics point of view and it favours higher H_2 production as compared to other sorbents such as Li_2ZrO_3, K-doped Li_2ZrO_3, Na_2ZrO_3 and Li_4SiO_4. Stability of CaO is a key issue for the fixed-bed sorption enhanced reactor technology. A drop of the re-carbonation extent for a pure CaO in re-carbonation/decomposition cycles is well-recognized. The main reasons for the decay of CO_2 capture capacity of CaO are pore blockage and sorbent sintering. However, the study of Alvarez et al. [11] revealed that the pore blockage is negligible for the 100 cycles at shorter carbonation times and sintering remains the main factor of capacity loss.

According to Molinderet al. [12], CaO undergoes three different reactions. CaO is highly hydroscopic and below 400 °C it undergoes CaO hydration reaction (**R1**). Then this reaction proceeds towards $Ca(OH)_2$ carbonation reaction (**R2**).

$$CaO_{(s)} + H_2O_{(g)} \leftrightarrow Ca(OH)_{2(s)} \Delta H_{298K} = -109.18 \text{kJ mol}_{CaO}^{-1} \tag{R1}$$

$$Ca(OH)_{2(s)} + CO_{2(g)} \leftrightarrow CaCO_{3(s)} + H_2O_{(g)} \Delta H_{298K} = -64.14 \text{ kJ mol}_{Ca(OH)2}^{-1} \tag{R2}$$

Fernández et al. [13] developed a mathematical model of SE-SMR process in a fixed bed reactor using Ca/Cu looping process and CaO as the sorbent and studied the effect of operating variables, such as catalyst to sorbent ratio, space velocity, S/C, pressure and temperature, on the composition of product gases. They used the experimental work of Lee et al. [14] for their model validation. Koumpouras et al. [15] developed a mathematical model and investigated the effect of sorbent on CH_4 conversion in a fixed bed reformer. Three cases were considered to investigate the effect of sorbent. In the first case, no sorbent was used so it represented a conventional SMR process. In the second case, sorbent was used but its ability to adsorb CO_2 was set to zero. So in this case, it only acted as a heat carrier. In the third case, sorbent was used as a heat carrier as well as CO_2 acceptor. It was found that a highest CH_4 conversion along the length of the reactor was obtained in third case. Ding et al. [16] and Xiu et al. [17] developed models of SE-SMR process and validated model predictions against their own experimental data.

In the literature, the mathematical model of SE-SMR process, under the industrial conditions has not been reported. In this paper, one dimensional heterogeneous mathematical model of SE-SMR process is developed and implemented in gPROMS model builder 4.1.0®. The predictions of reactor model are validated against the modelling data published by Fernández et al. [13]. The model predictions are also compared with the equilibrium data generated on an independent equilibrium based software (Chemical equilibrium and application software).

2. Mathematical modelling

A 1-D heterogeneous mathematical model of the SE-SMR process in an adiabatic packed bed reactor has been developed using gPROMS. This model accounts for the mass and energy transfer in both gas and solid phase. In this model it is assumed that;

a) The flow pattern of the gas phase in the packed bed reactor isa non-ideal plug flow in nature.

b) The temperature and concentration variations along the radial direction of reactor are considered negligible.

c) The active surface of the catalyst and sorbent facilitate the reforming and sorption reactions.

d) Ideal gas behaviour is applicable.

e) The process is adiabatic in nature.

f) The size of the catalyst and sorbent are uniform throughout the packed bed.

g) The porosity of the packed bed is constant.

2.1 Governing equations

The SMR reaction (**R3**) is highly endothermic in natureand non-equimolar (more products molesare formed than the reactants), so both high temperature and low pressure favour this reaction at equilibrium. On the other hand, the WGS reaction (**R4**) is exothermic and equimolar and is therefore favoured by low temperature, while its equilibrium is not pressure dependent. As the reforming reactions proceed and CO_2 is released, a CaO material captures this CO_2 gas by chemisorption producing solid $CaCO_3$. This sorption of CO_2 favours the formation of more H_2 by shifting the equilibrium of the WGS reaction and, via the resulting

enhanced CO consumption, also that of the SMR reaction towards more conversion of CH$_4$.

In this model, only CO$_2$ is considered to be adsorbed on the surface of the sorbent. The

adsorption of CO$_2$ on the surface of CaO is a highly exothermic carbonation reaction above

400 °C (**R5**);

$$CH_{4(g)} + H_2O_{(g)} \leftrightarrow CO_{(g)} + 3H_{2(g)} \qquad \Delta H_{298K} = 206 \text{kJ mol}_{CH4}^{-1} \qquad \text{(R3)}$$

$$CO_{(g)} + H_2O_{(g)} \leftrightarrow CO_{2(g)} + H_{2(g)} \qquad \Delta H_{298K} = -41 \text{ kJ mol}_{CO}^{-1} \qquad \text{(R4)}$$

$$CaO_{(s)} + CO_{2(g)} \leftrightarrow CaCO_{3(s)} \qquad \Delta H_{298K} = -178.8 \text{ kJ mol}_{CO}^{-1} \qquad \text{(R5)}$$

The overall SE-SMR reaction is slightly exothermic in nature as shown in **R6**;

$$CaO_{(s)} + CH_{4(g)} + 2H_2O \leftrightarrow CaCO_{3(s)} + 4H_{2(g)} \qquad \Delta H_{298K} = -13.9 \text{ kJ mol}_{CaO}^{-1} \qquad \text{(R6)}$$

On the basis of the assumptions reported above, the mathematical equations for mass and

energy balances within the reactor filled with sorbent and catalyst particles are listed in **Table**

1. The equations used to calculate the physical properties and model parameters are listed in

Appendix A.

Table 1: Summary of mass and energy balance equations used in the 1-D heterogeneous packed bed

reactor model

Mass and energy balances in the gas phase for reforming process;
$\varepsilon_b \left(\dfrac{\partial C_i}{\partial t} \right) + \dfrac{\partial (uC_i)}{\partial z} + k_{g,i} a_v (C_i - C_{i,s}) = \varepsilon_b D_z \dfrac{\partial^2 C_i}{\partial z^2}$ (1)
$\varepsilon_b \rho_g C_{pg} \left(\dfrac{\partial T}{\partial t} \right) + u \rho_g C_{pg} \dfrac{\partial (T)}{\partial z} = h_f a_v (T_s - T) + \lambda_z^f \dfrac{\partial^2 T}{\partial z^2}$ (2)
Mass and energy balance in the solid phase;
$k_{g,i} a_v (C_i - C_{i,s}) = \upsilon \rho_{cat} r_i - (1 - \upsilon) \rho_{ads} r_{ads}$ (3)

$$\rho_{bed}C_{p,bed}\left(\frac{\partial T_s}{\partial t}\right) + h_f a_v(T_s - T)$$

$$= \upsilon\rho_{cat}\sum -\Delta H_{rxn,j}\,\eta_j R_j + (1-\upsilon)\,\rho_{ads}\sum -\Delta H_{ads}\,r_{ads} \qquad (4)$$

Pressure drop calculations across the reactor bed;

$$\frac{\Delta P g_c}{L} = \frac{150}{d_p^2}\left[\frac{(1-\varepsilon)^2}{\varepsilon^3}\right]\mu u + \left(\frac{1.75}{d_p}\right)\left(\frac{1-\varepsilon}{\varepsilon^3}\right)\rho_g u^2 \quad (5)$$

In **Table 1**, υ is the ratio of the amount of the catalyst to the amount of sorbent filled in the packed bed reactor. r_{ads} is the rate of the adsorption of the CO_2. In literature, many expressions have been reported to describe the carbonation kinetics of CaO-based sorbents [13, 14, 18]. Lee et al. [14] performed experiments in a tubular reactor having an inner diameter 22 mm and a bed length of 290 mm containing 16.4 g Ni based reforming catalyst and 83.6 g CaO based sorbent. Through series of experiments in temperature range of 650-750°C, they determined the carbonation conversion data. In the past, many efforts were made to describe the kinetics of CO_2 adsorption on the surface of CaO based sorbent [14, 18-20]. Rodriguez et al.[21] proposed a first-order carbonation reaction rate and developed arate equation for CO_2 adsorption on the surface of CaO sorbent.

$$\frac{dq_{CO2}}{dt} = k_{carb}(X_{max} - X)\left(\upsilon_{CO2} - \upsilon_{CO2,eq}\right) \qquad (6)$$

Where X_{max} is the maximum conversion of CaO, kcarb [s^{-1}] is the reaction rate constant of active CaO sorbent and $\upsilon_{CO2,eq}$ is the volume fraction of CO_2 in equilibrium and it is given as[19];

$$\upsilon_{CO2,eq} = (4.137 \times 10^7)\exp\left(\frac{-20474}{T}\right) \qquad (7)$$

Where, X is the carbonation conversion of CaO. Dedmanet al. [22] reported that the carbonation rate of CaO is zero order with respect to CO_2 partial pressure. Bhatia et al.[20] proposed the carbonation rate expression which was independent of partial pressure of CO_2.Lee et al.[14] performed TGA analysis and determined the maximum conversion of active CaO at different temperatures. The experimental data revealed that the conversion of CaO was very low even at a high temperature (750 °C). This may be due to the large size of the CaO particles and low surface area. It was observed that using large size of the pellet, there was no sign of particle deterioration even after many cycles of carbonation and calcination. An expression to calculate the maximum conversion of CaO at any given temperature is given by:

$$X_{max} = 96.34\exp\left(\frac{-12171}{T}\right) 4.49\exp\left(\frac{4790.6}{T}\right) \tag{8}$$

The rate equations, reaction rate constants and equilibrium constants used in this model are given in **Appendix B**. On the basis of reactions involved in SE-SMR, the rate of formation or consumption of component i is given as;

$$r_i = \sum_{j=1}^{3} \eta_i \, \varphi_{ij} R_j \qquad i = CH_4, CO, CO_2, H_2 \text{ and } H_2O \tag{9}$$

Where η_j is the effectiveness factor of reaction j, φ_{ij} is the stoichiometric coefficient of component i in reaction j, and φ_{ij} is negative for reactants and positive for products.

The reactor model equations (Eqs. 1-4) consist of linear and non-linear partial differential equations (PDEs) and algebraic equations. The initial and boundary conditions used in solving these equations are as follows;

Boundary conditions;

At z = 0

$$C_i = C_{i,in} \qquad ; \qquad T = T_{in} \qquad ; \qquad T_s = T_{s,in} \qquad ; \qquad P = P_{in}$$

At z = L

$$\frac{\partial C_i}{\partial z} = 0 \qquad ; \qquad \frac{\partial T}{\partial z} = 0 \qquad ; \qquad \frac{\partial T_s}{\partial z} = 0$$

Initial conditions;

$$C_i = C_{i,0} \qquad ; \qquad T = T_o \qquad ; \qquad T_s = T_{s,o} \qquad ; \qquad q_{CO2} = 0$$

At initial conditions, it was considered that no gas was present within the reactor so the concentration of gas species was zero at the start i.e. at t = 0. But setting the concentration of H_2 zero made the rates of reforming reactions infinite (B.1-3). To avoid this, a very small initial concentration ($\sim 10^{-6}$) of the H_2 was used in the solution.

The first-order backward finite difference method (BFDM) was used to solve the PDEs using gPROMS. In this software, the differential algebraic solver (DASOLV) was used to convert the PDEs into the ordinary differential equation (ODEs), and a 4th order Runge-Kutta technique was used to solve the system of ODEs. The reactor was axially discretised into a number of intervals and the sensitivity of the model was first checked for discretization ranging from 10-1000 intervals. The model predictions were found independent of the number of intervals. Finally, the reactor was axially discretized by 100 uniform intervals for this paper and the output results were reported after every second.

3. Results and discussion

3.1 Model validation

The developed reactor model of SE-SMR process was first validated against the modelling results reported by Fernández et al. [13]. In addition, modelling results for the process were compared independently with equilibrium results generated by chemical equilibrium and applications (CEA) software [44, 45]. The reactor geometrical parameters such as length of packed bed(L), catalyst particle size (d_p), bed porosity (ε_b) and process variables like; S/C, operating temperature, pressure and mass flux (G_s) are adapted according to the values

reported by Fernández et al. [13]. In this work, the temperature range of 923-1023K, pressure range of 1.0-35bar, S/C of 3-7 and residence time between $0.1s^{-1}$ and $0.38s^{-1}$ were used. The values used for reactor parameters and operating variables are listed in **Table 2**.

Table 2: Physical parameters and operating conditions used in reactor model validation[13]

Reactor characteristics and operating conditions	
Gas feed temperature, $[T_{in}]$	923K
Initial solid temperature, $[T_o]$	923K
Wall temperature, $[T_w]$	1073 K
Total pressure, $[P]$	35bar
Steam to carbon ratio, $[S/C]$	5.0
Intel gas mass flux, $[G_s]$	$3.5 \ kgm^{-2}s^{-1}$
Maximum fractional carbonation conversion of CaO, $[X_{max}]$	0.4
Apparent density of reforming catalyst, $[\rho_{cat}]$	$550 \ kgm^{-3}$
Apparent density of CaO based sorbent, $[\rho_{CaO}]$	$1125 \ kgm^{-3}$
Diameter of particles, $[d_p]$	0.01 m
Reactor bed length, $[L]$	7 m
Bed porosity, $[\varepsilon_b]$	0.5

The overall production of H_2, conversion of CH_4 and CO_2 capture in the SE-SMR process depends upon the chemistry of the reactions taking place within the reactor and the

chemisorption characteristics of the sorbent. The adsorption of CO_2 on the surface of sorbent is highly exothermic reaction and it causes a gradual rise in the temperature of the system. On the other hand, the overall SMR process is endothermic in nature and needs heat to proceed. The gas temperature variation results obtained from the reactor model developed in this work were compared with modelling values reported by Fernandez et al. [13] and an excellent agreement is observed, as shown in **Figure 1.**
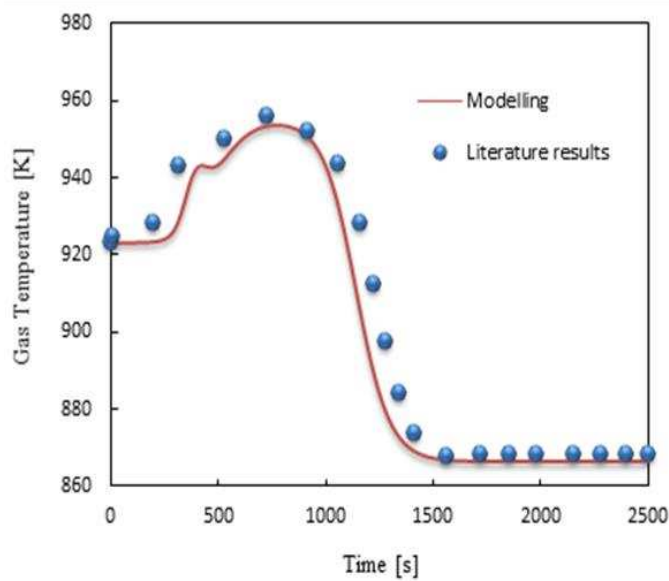

Figure 1: Predicted temperature profiles at the outlet of reactor at a feed temperature of 923K, S/C of 5.0, 35 bar and gas mass flow velocity of 3.5 kg m^{-2}s^{-1} under adiabatic conditions. Dots are literature values [13] andsolid linerepresents modelling results of this study.

In the pre-breakthrough period (t<720s), rise in the outlet gas temperature is observed because of the CO_2sorption process. In this period, adsorption of CO_2 is maximum as the rate of carbonation reaction is high. The maximum temperature obtained in this work is 953.7K i.e. an increase of 30.7K from the feed temperature, while a rise of 32K above the feed temperature is reported in the modelling from the literature [13].

In the breakthrough period (720s ≤ t ≤ 1500 s), a drop in temperature is observed, but after 1500s the temperature becomes constant. The minimum temperature reached is 866.3 K i.e. a decrease of 56.7 K from feed temperature compared to a drop of 55 K [13]. The sorbent is not active in the post-breakthrough period and only SMR process is happening in this period, hence the overall process is endothermic and the temperature of the adiabatic systemdrops from 923K to 866.3K.

Fernandez et al.[13] also reported the modelling of the SE-SMR undernon-adiabatic conditions.For the non-adiabatic SE-SMR process, the energy balance equation wasmodified and the transfer of heat from the wall to the process gas was included. The modified energy balance equation is given by;

$$\rho_{bed}C_{p,bed}\left(\frac{\partial T_s}{\partial t}\right) + h_f a_v(T_s - T)$$

$$= \upsilon\rho_{cat}\sum -\Delta H_{rxn,j}\, \eta_j R_j + (1 - \upsilon)\rho_{ads}\sum -\Delta H_{ads}\, r_{ads} + h_w(T_w - T)\frac{4}{D_r}\,(10)$$

In this equation, h_w is the heat transfer coefficient atthe wall of the reactor, T_w is the temperature of the reactor wall and D_r is the inner diameter of the reactor. The modelling results of this work and the results of Fernandez et al.[13]under the same operating conditions for non-adiabatic process are compared in **Figure 2** and a good agreement is observed.
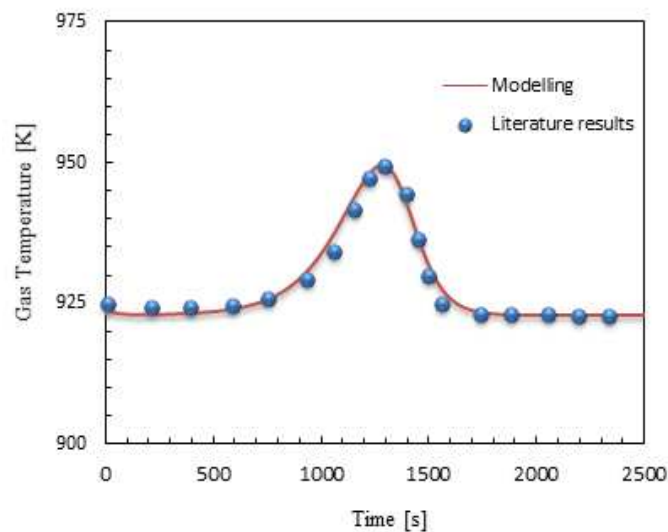
Figure 2: Predicted gas temperature profiles at the outlet of reactor at a feed temperature of 923K, S/C of 5.0, 35 bar and gas mass flow velocity of 3.5 kg m^{-2}s^{-1} under non-adiabatic conditions. Dots are literature values [13] and solid line represents modelling values of this study.

By analysing both adiabatic and non-adiabatic processes, it is observed that in the pre-breakthrough period of the adiabatic process temperature is higher than the temperature in the non-adiabatic process. This higher temperature results in more CO_2 production and hence the carbonation rate is maximum. The higher carbonation rate thus makes the duration of pre-breakthrough shorter in the adiabatic process as compared to the non-adiabatic process. Although the rise of temperature is the same in both cases, the shorter pre-breakthrough period of the adiabatic process is more favourable under fast cycling operations. On this basis, the adiabatic process is selected for further analysis.

The reaction rate constant of CaO (k_{carb}) plays a major role in the kinetics of carbonation reaction (**R5**). The effect of carbonation reaction rate constant on the temperature profile of the SE-SMR under the adiabatic conditions was studied by Fernandez et al.[13]. Their findings are used to validate the modelling results. In **Figure 3,** three rate constants are used and it is quite clear that the reactor temperature is dependent on the value of carbonation rate constant. For a smaller value of carbonation rate constant (k_{CO2} = 0.18 s^{-1}), the pre-breakthrough period is longer (~1500s) than higher values of k_{CO2} (~500s). The lower value of k_{CO2} suggests that the sorbent is not highly reactive and the rate of CO_2 adsorption is slow. While in the case of higher value of k_{CO2} (0.7s^{-1}), the rate of CO_2 adsorption on the surface of sorbent is very fast and hence the sorbent reached its full absorption capacity earlier. The higher value is preferable for fast cycles of SE-SMR process. For the three different values of carbonation rate constant, the final temperature of the system is the same i.e. 867.9K as this is determined by the adiabatic conditions and post-breakthrough conditions of SMR.
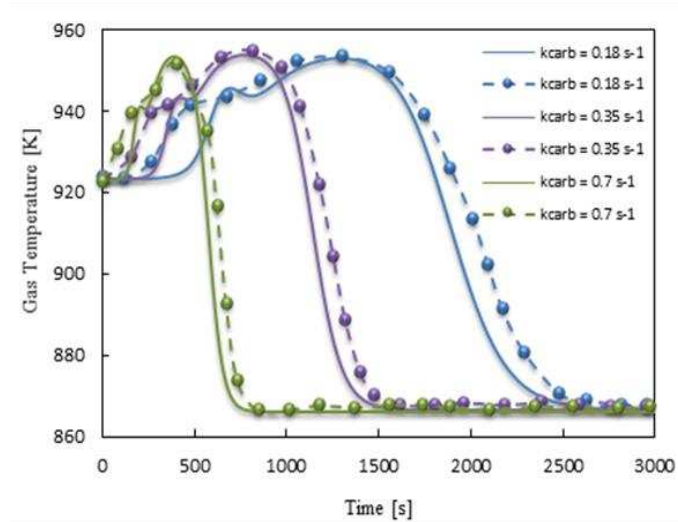
Figure 3: The effect of carbonation rate constant on the gas temperature profile at the outlet of reactor at a feed temperature of 923K, S/C of 5.0, 35 bar and gas mass flow velocity of 3.5 kg m^{-2}s^{-1} under adiabatic conditions. Dotted lines are literature values [13] and solid lines are modelling results of this study.

3.2 Sensitivity analysis of SE-SMR model

The optimum operating conditions for the SE-SMR process were determined by evaluating the process performance under various conditions of temperature, pressure, S/C and gas mass flow velocity. The simulation resultsobtained using the reactor modelare also compared with the equilibrium results generated using CEA software.

3.2.1 Methodology of equilibrium calculationsusing CEA

The CEA software was used to generate the equilibrium data [44, 45]. This software is based on minimization of Gibbs free energy (G) [46]. The chemical equilibrium analysis was done by considering the gas species involved in the reactant and product streams, which are CH_4, H_2, CO, CO_2, H_2O, N_2, CaO and $CaCO_3$, using the option 'ONLY' in the CEA software. This

allows specification of a restricted pool of species as potential equilibrium products. The calculations of individual equilibrium molar outputs were performed on the basis of N_2 balance, which allowed the determination of the total moles of product at equilibrium in post processing, and its product with the relevant mole fractions predicted by the CEA output. The solid carbon equilibrium product was not included as it is not significant in conditions of excess stoichiometric steam of the present study.To study the effect of temperature, pressure and S/C were fixed and the CEA code runs in temperature-pressure (tp) mode, corresponding to an isothermal and isobaric process. Similarly, to study the pressure effect; temperature and S/C conditions were fixed, still in tp mode.

3.2.2 Effect of temperature

The conventional SMR process is carried out in industry under high temperature (800-1000°C) and high pressure (20-35bar) conditions [23, 24]. The SE-SMR process is simulated under various temperatures (500-800 °C) but at a pressure of 30 bar, Ca/C of 1 and S/C of 3 using the CEA software.From the equilibrium results generated usingCEA it is concluded that 99% conversion of CH_4 is achieved at a high temperature between 700-800°C, S/C of 3.0, 1bar and Ca/C of 1.0. But at such a high temperature, H_2 purity is just 76% because the CO_2 capture efficiency is almost zero at such a high temperature conditions. So there is a trade-off between the conversion of CH_4 and H_2 purity.

In **Figure 4,** the effect of temperature on CH_4 conversion, H_2 purity and yield (wt. % of CH_4) and CO_2 capture efficiency is presented. The simulation results generated using gPROMS are compared with the equilibrium results generated using CEA to provide the maximum conversion and H_2 yield values permitted by equilibrium in the same conditions.

A CH_4 conversion of 69.7% was achieved at 973K (72.7% at equilibrium). The higher conversion of CH_4 at 973K results in higher yield of H_2 i.e. 27.6%(wt. % of feed CH_4), but

lower CO_2 capture efficiency. As temperature is increased from 973K to 1050K, the drop in H_2 purity drops from 83.4% to 76.6%, caused by lower CO_2 capture efficiency.This shows that the carbonation reaction (R5) is not active at temperature higher than 973 K, hence a drop in CO_2 capturing efficiency results in more CO_2 in the product, reducing the partial pressure of the reforming reactants. Therefore, a drop in H_2 is observed after 973 K. In **Figure 4(d)**, the drop in CO_2 capturing is higher after 973K in modelling results as compared to equilibrium results. This steep drop is because of the carbonation kinetic values used in the modelling are not favourable at such a high temperature. The optimum temperature range for the SE-SMR process at 30 bar and S/C of 3.0, Ca/C of 1 and gas mass flow velocity of 3.5 kg $m^{-2}\,s^{-1}$ is 873-973K. This range is used for further modelling studies.
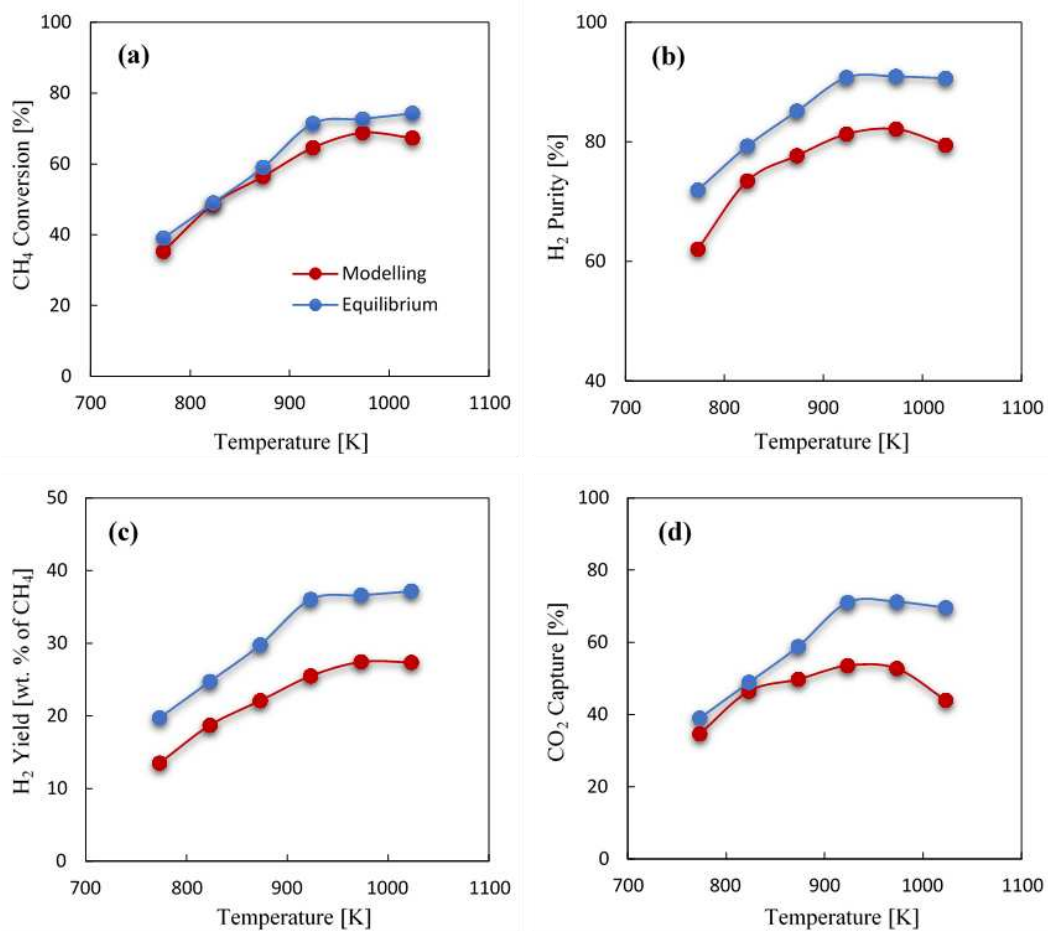
Figure 4: The effect of temperature on the a) CH_4 conversion; b) H_2 purity; c) H_2 yield (wt. % of CH_4) and d) CO_2capture efficiency at 30bar, S/C of 3.0, CaO/C of 1.0 and gas mass flow velocity of 3.5 kg $m^{-2}s^{-1}$

In **Figure 5,** dynamic profiles of dry mole percent of H_2 and CO_2 in the temperature range of 873-973K are presented. The activity of sorbent was higher at lower temperatures (873K and 923K) and as the temperature increased beyond 923K, the activity of sorbent decreased. Thepre-breakthrough period in the case of 873K and 923K was smaller than that of 973 K. The higher activity of sorbent made the system with a lower temperature of 873 K preferable in fast cyclic operation as high capacities were reached faster and were less limited by the equilibrium maximum. The mole percent of CO_2 and H_2 in the pre-breakthrough period for the SE-SMR process having 973K as feed temperature were 2.9% and 84.1% respectively. By comparison at 923K feed temperature, the mole percents of CO_2 and H_2were 0.34% and 87.3% respectively.
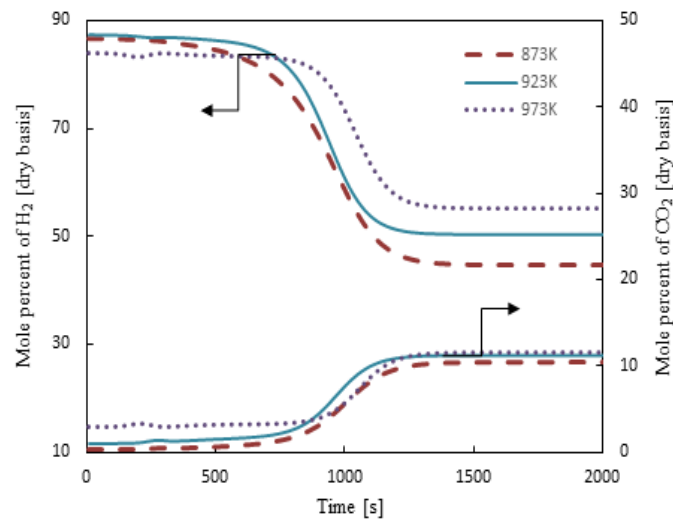

Figure 5: Composition profile of H_2 and CO_2 on dry basis at T=873-973K, 30bar, S/C of 3.0 and gas mass flow velocity of 3.5kg $m^{-2}s^{-1}$

The modelling results presented in **Figure 4** and **5** show that 923K is the optimum temperature in terms of CH_4 conversion, H_2 purity and yield, CO_2 capture efficiency and sorbent activity for the SE-SMR process operating under 30bar and S/C of 3.0.

3.2.3 Effect of pressure

Temperature has a positive effect on the dynamics of the reforming process as seen in previous section, but according to Le-Chatelier's principle pressure has a negative equilibrium effect on the reforming process. Pressure has a positive effect on the kinetics of CO_2 sorption capture, as adsorption of CO_2 on the surface of sorbent is favourable at a pressure higher than 1bar [25]. In industrial processes, high pressure H_2 is required downstream of reformer and it is ill advised to generate H_2 at a low pressure and then use energy intensive compressors to pressurise it according to required storage conditions [26].

In the previous section, 923K is selected as an optimum temperature. So, the effect of pressure on the SE-SMR is studied at this constant temperature. In **Figure 6(a-d)**, it is observed that with the increase in pressure from 20 to 35 bar the conversion of CH_4 reduces from 73.5% to 64.8% and same is the case with H_2 purity and CO_2 capture i.e. both reduce from 86.5 to 82.9% and 64.5 to 58.8% respectively in the reactor model.

The dynamic behaviour of the SE-SMR process under different operating pressure conditions is presented in **Figure 6 (a-d).** At 20 bar and S/C of 3.0, CH_4 conversion is 73.5%. To study the process atan industrial scale, 30bar is used and at this pressure the equilibrium CO_2capture efficiency and H_2 purity is 71.0% and 90.8% respectively. Underthe same operating conditions, the reactor model yields 60.8% CO_2capture efficiency and 84.1% H_2 purity as shown in **Figure 6 (c & d)**.
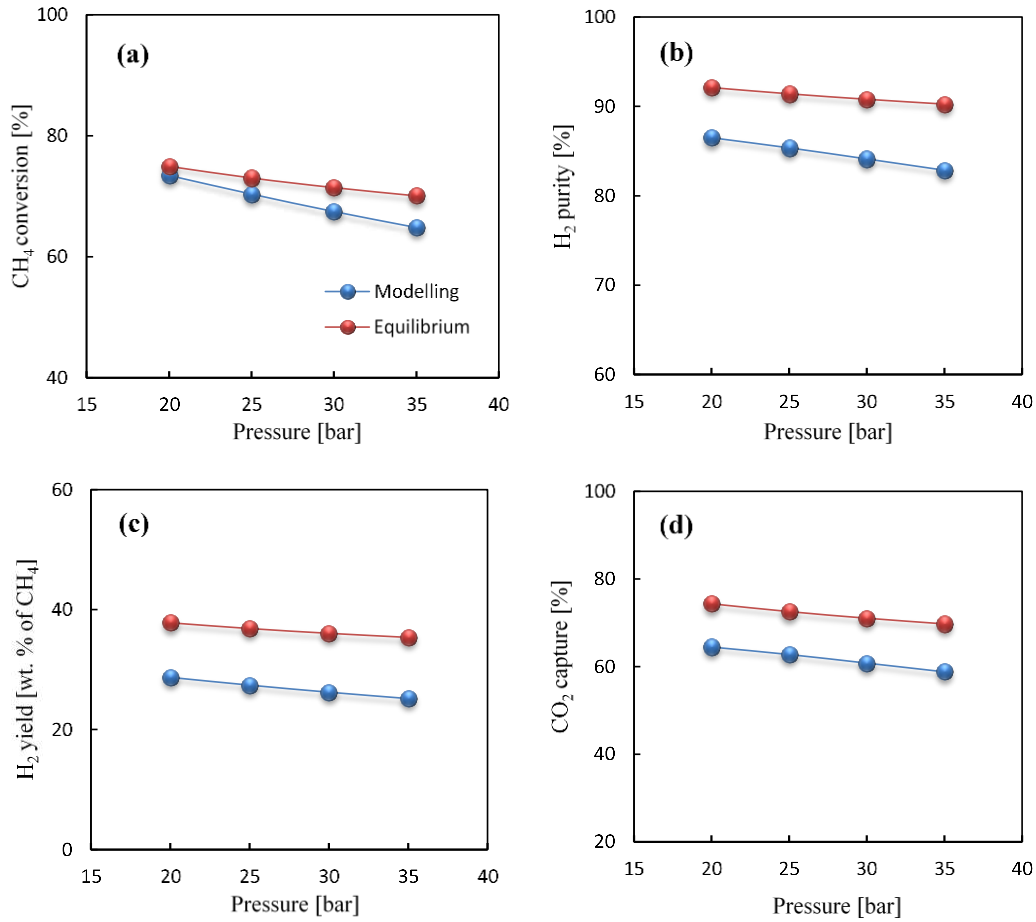
Figure 6: The effect of pressure on the a) CH_4 conversion; b) H_2 purity; c) H_2 yield (wt. % of CH_4) and d) CO_2 capture efficiency at 923 K, S/C of 3.0, CaO/C of 1.0 and gas mass flow velocity of 3.5 kg $m^{-2} s^{-1}$

The CO_2 capture efficiency varies with pressure because pressure has a significant effect on the rate of adsorption of CO_2 on the active site of the CaO based sorbent. In **Figure 7,** the effect of pressure on the carbonation rate is illustrated. The rate of carbonation is higher at 20bar, hence more capture of CO_2 is expected at this pressure as compared to pressure higher than 20 bar. The maximum value of carbonation rate for 20 and 35 bar is 7.63×10^{-4} and 6.27×10^{-4} mol kg^{-1} s^{-1} respectively. This shows that the carbonation rate is almost 1.2 times higher in the case of 20 bar than 35 bar. The pre-breakthrough period at 20 and 35 bar is 600s and 700s respectively. So the sorbent reaches its maximum activity much earlier at 20 bar than 35 bar.
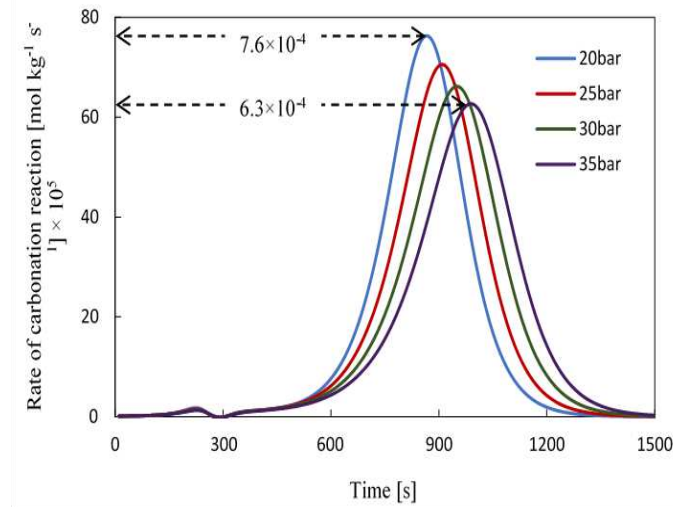
Figure 7: The effect of pressure on the rate of carbonation at 923K, S/C of 3.0, CaO/C of 1.0 and gas mass flow velocity of 3.5 kg m^{-2}s^{-1}

3.2.4 Effect of S/C

One of the vital parameters in the performance of SE-SMR process is S/C. The comparison of modelling and equilibrium results in terms of CH_4 conversion, H_2 purity and yield (wt. % of CH_4) andCO_2capture efficiencyare presented in **Table 3** for S/C from 1 to 3, and dynamic profiles of H_2 and CO_2 mole% are shown in **Figure 8** for S/C up to 6.

Table 3: Effect of S/C on the CH_4 conversion, H_2 yield (wt. % of CH_4), H_2 purity and CO_2capture efficiency at 923K, 30bar and gas mass flow velocity of 3.5 kg m^{-2}s^{-1}

S/C	CH_4 Conversion [%]	H_2 yield [wt.% of CH_4]	H_2 purity [%]	CO_2 capture [%]
1	M : 32.4	M : 12.5	M : 58.5	M : 28.9

	E : 34.4	E : 17.4	E : 67.6	E : 34.0
2	M : 51.7	M : 20.0	M : 74.7	M : 46.1
	E : 56.2	E : 28.3	E : 83.5	E : 55.8
3	M : 67.5	M : 26.2	M : 84.1	M : 60.8
	E : 71.4	E : 36.1	E : 90.8	E : 71.0

Where; M: gPROMS modelling results and E: Equilibrium results generated via CEA

Tabulated results show that the higher S/C is favourable for higher conversion of CH_4. In the S/C range 1to 3, the maximum conversion of CH_4 and H_2 purity are achieved at S/C of 3.0. It is quite clear from the results in **Figure 8** that more steam enhances the purity of H_2 (74.7% to 97.5% as S/C increases from 2 to 6). The higher amount of steam in the SE-SMR process enhances the selectivity of H_2 and the lower amount of CO_2slows down the carbonation rate. Ascan be seen in **Figure 8**, the pre-breakthrough period is shorter for S/C of 2 as compared to the process having a higher S/C. The pre-breakthrough periods for the process having S/C of 2 and 6 were 600s and 1000s respectively. It is concluded from the results that higher S/C is preferred for higher purity of H_2, CH_4 conversion and H_2 yield althoughthis would reduce the thermal efficiency of the process as more heat is required for the generation of the excess steam. Since there is always a trade-off between the H_2 purity/yield and the thermal efficiency of the process, in industrial SMR processes, S/C of 3.0 is common [27].
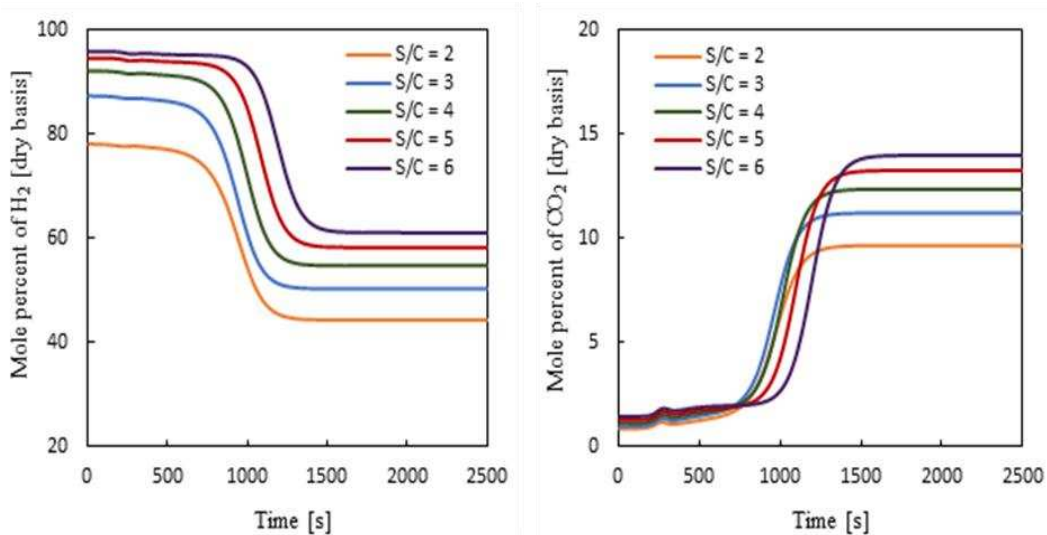
Figure 8: Dynamic profile of H_2 and CO_2 composition (dry basis) at the outlet of reactor for various S/C (2-6) under the adiabatic conditions at 923K, 30bar and 3.5kg m^{-2}s^{-1} gas mass flow velocity

Fernandez et al.[28] modelled the SE-SMR process for Ca/Cu looping system and they studied the variation of temperature at the exit of the reactor for various S/C. They found that temperature variation is almost negligible for S/C range of 2 to 6 and the length of the pre-breakthrough period changed from 600 s to 1000 s. In **Figure 9**, the dynamic profile of temperature generated in this work is presented for S/C of 2 to 6 and it is in excellent agreement with literature results. At the start there is a rise in the temperature, it is because of the exothermicity of the SE-SMR process. The rise in temperature for all S/C (2 to 6) is about 20K from the feed temperature. As expected from previous results, the pre-breakthrough period in case of higher S/C is longer than the lower S/C.

The minimum temperature was reached in the post-breakthrough period when all the sorbent was saturated. In the post-breakthrough period, only conventional SMR process took place. For all S/Cin the range studied, the minimum temperature achieved was 881K i.e. drop of 42K from the feed temperature. Fernandez et al.[13]used 35bar and reported a minimum temperature of 868 K in the post-breakthrough period.
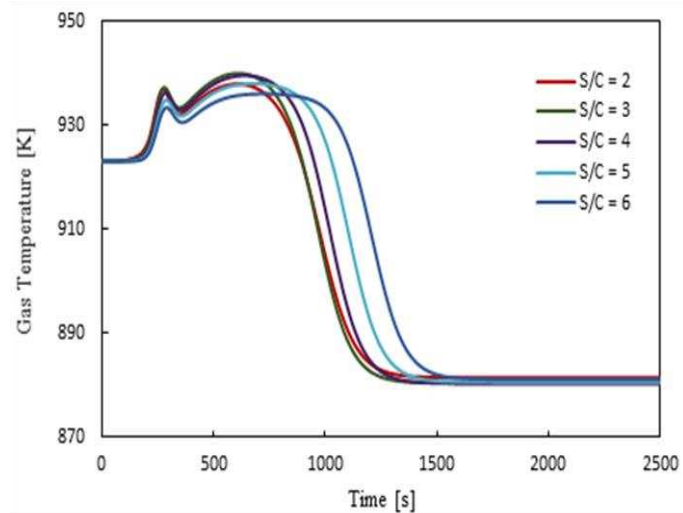
Figure 9: Dynamic profiles of temperatures at the exit of reactor for various S/C at 30bar, 923K feed temperature and 3.5kg $m^{-2}s^{-1}$ gas mass flow velocity

3.2.5 Effect of gas mass flow velocity

The gas mass flow velocity (G_s) is another important operating variable that affects the performance of the system. The selection of $G_s$is highly dependent upon the length of the reactor. Rostrup et al.[29] proposed 1.5-2 m s^{-1} velocity as the optimum velocity to get the conversion of CH_4 close to the equilibrium conditions.

In this work, various values of$G_s$are used to study the effect on the performance of the SE-SMR process. In **Figure 10**, the dynamic variation of CO_2 and H_2 composition (dry basis) is presented under the operating conditions of 923 K, 30 bar, S/C of 3.0 and various G_s (2 to 7 kg m^{-2} s^{-1}). The lower G_s resulted in a longer pre-breakthrough period as the residence time ishigher in the reactor and a higher conversion of CH_4 is achieved. For G_s of 2 kg $m^{-2}s^{-1}$, the conversion of $CH_4$was 71%. This was very close to equilibrium value of 71.4% under the same operating conditions. As G_s increased, the CH_4 conversion decreased because of shorter residence time. The longer pre-breakthrough periods for lower G_s may be unsuitable for fast cyclic processes. The pre-breakthrough period increased from 90s to 1200s as $G_s$decreased

from 7 kg m^{-2}s^{-1}to 2 kg m^{-2}s^{-1}. The optimum G_s selected was 3.5 kg m^{-2}s^{-1}due to having a pre-breakthrough period of 700s. At this G_s,CH_4 conversion and H_2 purity is 67.5% and 84.2% respectively, corresponding to 71.4% and 90.8% atequilibrium.
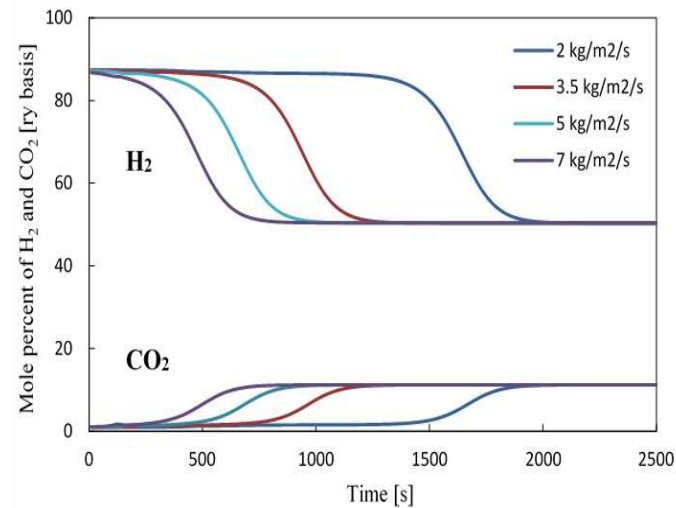

Figure 10: Dynamic profile of H_2 and CO_2 composition (dry basis) at the outlet of reactor for various $G_s$under the adiabatic conditions, at 923K, 30bar and S/C of 3.0

3.3 Comparison of SE-SMR and SMR models

To compare the performance of the SE-SMR process with a conventional SMR process, optimum values obtained through sensitivity analysis in previous sections are used.

In **Figure 11,** the effluent composition (dry basis) profiles are presented for the SE-SMR and SMR processes under the operating conditions of 923K, 30bar, S/C 3.0 and G_s of 3.5 kg m^{-2}s^{-1}. The compositions of H_2 and CO_2 at equilibrium under the same operating conditions are also presented in this figure. Modelling results show that the composition of CO_2 was almost zero up to 700s in the SE-SMR and after t $\geq$1500s (~25 min), the CO_2 compositions in SMR and SE-SMR became equal. In the CO_2 pre-breakthrough period, the compositions of H_2

is87% in SE-SMR but only 50% in SMR. In the CO_2 post-breakthrough period (t≥1500s), the sorbent was no longer active hence both SE-SMR and SMR processeshave the same CO_2 and H_2 compositions.
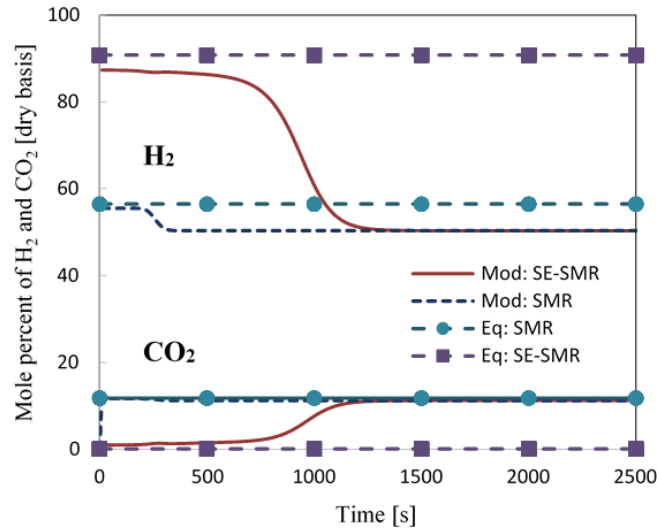

Figure 11: Effluent mole percent profiles of H_2 and CO_2 in SE-SMR and SMR process at 923K, 30bar, S/C of 3.0 and gas mass flow velocity of 3.5kg m^{-2}s^{-1}

The adsorption of CO_2 on the active site of the sorbent is highly exothermic and it releases considerable amount of heat (-178 kJ mol$_{CaO}^{-1}$). In adiabatic conditions this results in higher temperatures in the reactor bed for the SE-SMR, which is more favourable for the reforming reactions. The enhancement in conversion of CH_4 due to CO_2 sorption is calculated. The conversion enhancement reveals the advantage of using sorbent within the system as shown in **Figure 12 (a)**. The conversion enhancement factor E (t) is calculated as;

$$E(t) \ = \frac{(X_{CH4})_{ad} - (X_{CH4})_{nad}}{(X_{CH4})_{nad}} \times 100 \tag{11}$$

Where $(X_{CH4})_{ad}$ is the conversion of CH_4 in the presence of adsorbent (ad) and $(X_{CH4})_{nad}$ is the conversion of CH_4 in the absence of adsorbent (nad). The enhancement in conversion

decreases at breakthrough when the sorbent gets saturated. As it can be seen that conversion enhancement is zero in the post-breakthrough period.
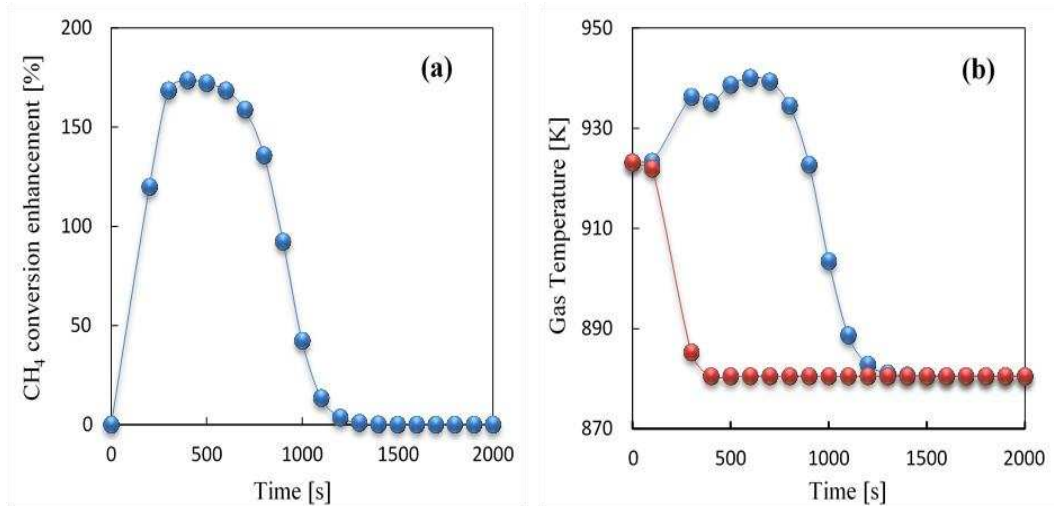

Figure 12: a) CH$_4$conversion enhancement and b) Comparison of temperature profiles generated at the exit of packed bed reactor in SE-SMR and SMRat 923K, 30bar, S/C of 3.0 and mass flow velocity of 3.5kg m^{-2}s^{-1}

The presence of sorbent with catalyst actually enhances the reforming reaction rates by increasing the temperature of the process. The comparison of temperature profile for both SE-SMR and SMR is also presented in **Figure 12 (b).**

4. Conclusion

The one-dimensional SE-SMR model developed using gPROMS mimics the modelling data reported in literature [13]and shows an excellent agreement. The mathematical model under both adiabatic and non-adiabatic conditions performs well according to the literature data. Operating parameters, such as; temperature, pressure, S/C and gas mass flow velocity have a strong influence on the performance of the SE-SMR process. The optimum temperature obtained under the high pressure (20 to 35 bar) conditions is 923 K. This temperature gives

67.5% CH_4 conversion at S/C of 3.0 and 30bar and the purity of H_2 achieved is 84.1%. The selection of optimum pressure for industrial scale is a trade-off between H_2 purity, plant capital cost and downstream pressure requirements. The pressure as high as 30bar is considered as optimum in this study as it fulfils the requirement of industrial pressure of H_2 and gives a considerable purity of H_2 (84.1%). Selection of optimum S/C is also a trade-off between the purity of H_2 and operational cost of the plant. The higher amount of steam enhances the conversion of CH_4 and gives more pure H_2 but high steam requirement is not feasible in terms of operational cost of the plant. S/C of 3.0 is selected to meet the requirements of H_2 purity at a minimum operational cost. The selection of gas mass flow velocity is done on the basis of operational time of the process and H_2 purity achieved at the outlet of the reactor. The gas mass flow velocity of 2 kg $m^{-2}s^{-1}$ induces onset of pre-breakthrough period at 1200s while in the case of gas mas flow velocity of 7 kg $m^{-2}s^{-1}$ this period is 90s. The gas mass flow velocity of 3.5 kg $m^{-2}s^{-1}$ is picked as an optimum value having a pre-breakthrough period of 700 s and 67.5% CH_4 conversion against the equilibrium conversion of 71.4%. Furthermore, the comparison between the predictions of the SE-SMR and SMR models shows enhancement of CH_4 conversion by 180% due to the presence of the sorbent in the reactor. The adsorption of CO_2 on the active surface of the sorbent is highly exothermic process and it releases considerable amount of heat (-178 kJ mol^{-1}). This heat promotes the reforming reactions and conversion above the conventional SMR process is achieved.

Acknowledgement

NOMENCLATURE

a_v	Interfacial area per unit volume of catalyst bed, m^2/m^3
C_i	Concentration of component i, mol/m^3
$C_{i,in}$	Inlet concentration of component i, mol/m^3
$C_{i,o}$	Concentration of component i at t=0, mol/m^3
$C_{i,s}$	Concentration of component i on solid surface, mol/m^3
C_{pg}	Heat capacity of gas at constant pressure, $J/(kg.K)$
$C_{p,bed}$	Heat capacity of bed at constant pressure, $J/(kg.K)$
D_i	Effective diffusion coefficient, m^2/s
D_m	Average molecular diffusivity, m^2/s
d_P	Catalyst particle diameter, m
D_r	Inner diameter of the reactor, m
D_z	Axial dispersion coefficient, m^2/s
E_j	Activation energy of reaction j, J/mol
$E(t)$	Conversion enhancement
G_s	Gas mass flow velocity, $kg/(m^2.s)$
h_f	Gas to solid heat transfer coefficient, $W/(m^2.s)$
$J_{D,i}$	Chilton-Colburn j-factor for mass transfer
J_H	Chilton-Colburn j-factor for heat transfer
k	Thermal conductivity, $W/(m.K)$
k_{eff}	Effective thermal conductivity, $W/(m.K)$
$k_{g,i}$	Gas to solid mass transfer coefficient of component i, m^3/m^2s
K_i	Adsorption constant of species i
k_j	Kinetic rate constant of reaction j

$K_{o,i}$	Reference adsorption constant of species i
K_j	Thermodynamic equilibrium constant of reaction j
k_z	Axial thermal conductivity, W/(m.K)
L	Packed bed length, m
p_i	Partial pressure of specie i, bar
P	Total pressure, bar
p_i^{feed}	Partial pressure of component i in feed, bar
P^o	Pressure at z=0, bar
P_{in}	Inlet pressure of the feed, bar
P_r	Prandtl number
q_{CO2}	Solid phase concentration of CO_2 (average on the surface of sorbent), mol/m^3
R, R_g	Ideal gas constant, J/(mol.K)
r_i	Rate of production of component i, mol/(kg$_{cat}$.s)
r_{ads}	Rate of adsorption of CO_2, mol/(kg.s)
R_e	Reynolds number
R_j	Rate of reaction j, mol/(kg$_{cat}$.s)
S_{ci}	Schmidt's number
T	Temperature within system, K
T_{in}	Inlet temperature, K
T_s	Temperature of catalyst particles, K
$T_{s,o}$	Temperature of solid particles at 't=0', K
T_w	Wall temperature, K
u_s, v	Superficial velocity, m/s
X_{max}	Maximum fractional carbonation conversion of CaO

X_{CH4}	Fractional conversion of CH_4
ΔH_{rex}	Heat of reaction at standard condition, J/mol
ΔH_{ads}	Heat of adsorption reaction at standard condition, J/mol
ΔP	Pressure drop across the reactor, bar
Greek Letters	
Ω	Denominator term in the reaction kinetics
λ_z^f	Effective thermal conductivity, W/(m.K)
λ_g	Average gas thermal conductivity, W/(m.K)
λ_s	Solid thermal conductivity, W/(m.K)
λ_z^o	Effective thermal conductivity of motionless fluid, W/(m.K)
ρ_f	Density of fluid, kg/m^3
ρ_{cat}	Density of catalyst, kg/m^3
ρ_{ad}	Density of sorbent, kg/m^3
η_j	Effectiveness factor of reaction 'j'
Φ_{ij}	Stoichiometric coefficient of component 'i' in reaction 'j'
μ_g	Viscosity of gas, Pa.s
υ	Ratio of catalyst amount to sorbent amount

APPENDIX A

Physical properties used in the reactor model are given as;

The axial mas dispersion coefficient is given as[30];

$$D_z = 0.73D_m + \frac{0.5u_s d_p}{1 + 9.49D_m/u_s d_p} \tag{A.1}$$

Where D_z is the axial dispersion coefficient (m²/s), d_p is the diameter of particle (m), u_s is the interstitial gas velocity (m/s) and D_m is the average molecular diffusivity (m²/s).

The effective thermal conductivity is given by the following relations[31];

$$\frac{\lambda_z^f}{\lambda_g}$$

$$= \frac{\lambda_z^o}{\lambda_g} + 0.75 Pr Re_p \tag{A.2}$$

$$\frac{\lambda_z^o}{\lambda_g} = \varepsilon_b + \frac{1 - \varepsilon_b}{0.139\varepsilon_b - 0.0339 + \left(\frac{2}{3}\right)\lambda_g/\lambda_s} \tag{A.3}$$

Where λ_g is the average thermal conductivity of gas (W m⁻¹ K⁻¹)and λ_s is the average thermal conductivity of solid material(W m⁻¹ K⁻¹). The mass transfer coefficient is given as[32];

$$k_{g,i} = j_{D,i} Re Sc_i^{1/3} \frac{D_i}{d_p} \tag{A.4}$$

$$\varepsilon_b j_{D,i} = 0.765 Re^{-0.82} + 0.365 Sc_i^{-0.398} \tag{A.5}$$

The dimensionless numbers are given as,

$$Re = \frac{\rho_f u_s d_p}{\mu} \qquad ; \qquad 0.01 < Re < 1500 \tag{A.6}$$

$$Sc_i = \frac{\mu}{\rho_f D_i} \qquad ; \qquad 0.6 < Sc < 7000 \ , \ \ 0.25 < \varepsilon_b < 0.96 \tag{A.7}$$

The heat transfer coefficient and its dimensionless numbers are given by the following relations [32, 33];

$$h_f = j_H \frac{C_{pg} G_s}{Pr^{2/3}} \tag{A.8}$$

$$j_H = 0.91Re^{-0.51}\psi \qquad ; \qquad 0.01 < Re < 50 \tag{A.9}$$

$$j_H = 0.61Re^{-0.41}\psi \qquad ; \qquad 50 < Re < 1000 \tag{A.10}$$

$$Pr = \frac{C_{pg}\mu_g}{\lambda_g} \tag{A.11}$$

APPENDIX B

The kinetic rate equations and kinetic data used for this modelling work are given as;

$$R_1 = \frac{k_1}{p_{H_2}^{2.5}}\left(p_{CH_4}p_{H_2O} - \frac{p_{H_2}^3 p_{CO}}{K_I}\right)\left(\frac{1}{\Omega^2}\right) \tag{B.1}$$

$$R_2 = \frac{k_2}{p_{H_2}}p_{CO}p_{H_2O} - \frac{p_{H_2}p_{CO_2}}{K_{III}}\left(\frac{1}{\Omega^2}\right) \tag{B.2}$$

$$R_3 = \frac{k_3}{p_{H_2}^{3.5}}\left(p_{CH_4}p_{H_2O}^2 - \frac{p_{H_2}^4 p_{CO_2}}{K_{II}}\right)\left(\frac{1}{\Omega^2}\right) \tag{B.3}$$

$$k_1 = k_{0,1}\exp\left(\frac{-E_1}{RT}\right) = (1.17 \times 10^{15})\exp\left(\frac{-240100}{RT}\right) \tag{B.4}$$

$$k_2 = k_{0,2}\exp\left(\frac{-E_2}{RT}\right) = (5.43 \times 10^5)\exp\left(\frac{-67130}{RT}\right) \tag{B.5}$$

$$k_3 = k_{0,3}\exp\left(\frac{-E_3}{RT}\right) = (2.83 \times 10^{14})\exp\left(\frac{-243900}{RT}\right) \tag{B.6}$$

$$K_I = \exp\left(\frac{-26830}{T_s} + 30.114\right) \tag{B.7}$$

$$K_{II} = \exp\left(\frac{4400}{T_s} - 4.036\right) \tag{B.8}$$

$$K_{III} = K_I K_{II} \tag{B.9}$$

$$\Omega = 1 + K_{CO}p_{CO} + K_{H_2}p_{H_2} + K_{CH_4}p_{CH_4} + K_{H_2O}\frac{p_{H_2O}}{p_{H_2}} \tag{B.10}$$

$$K_i = K_{oi}\exp\left(\frac{-\Delta H_i}{R_g T}\right) \tag{B.11}$$

REFERENCES

[1] Yang RT. Gas separation by adsorption processes: Butterworth-Heinemann; 2013.

[2] Mayorga SG, Hufton JR, Sircar S, Gaffney TR. Sorption enhanced reaction process for production of hydrogen. Phase 1 final report. Air Products and Chemicals, Inc., Allentown, PA (United States); 1997.

[3] Barelli L, Bidini G, Gallorini F, Servili S. Hydrogen production through sorption-enhanced steam methane reforming and membrane technology: a review. Energy. 2008;33:554-70.

[4] Metz B, Davidson O, De Coninck H, Loos M, Meyer L. IPCC special report on carbon dioxide capture and storage. Prepared by Working Group III of the Intergovernmental Panel on Climate Change. IPCC, Cambridge University Press: Cambridge, United Kingdom and New York, USA. 2005;4.

[5] Roger W. Hydrogen production. Google Patents; 1933.

[6] Brun-Tsekhovoi A, Zadorin A, Katsobashvili YR, Kourdyumov S. The process of catalytic steam-reforming of hydrocarbons in the presence of carbon dioxide acceptor. Hydrogen energy progress VII, proceedings of the 7th world hydrogen energy conference1988. p. 25-9.

[7] Hufton J, Mayorga S, Sircar S. Sorption-enhanced reaction process for hydrogen production. AIChE Journal. 1999;45:248-56.

[8] Ochoa-Fernández E, Haugen G, Zhao T, Rønning M, Aartun I, Børresen B, et al. Process design simulation of H2 production by sorption enhanced steam methane reforming: evaluation of potential CO2 acceptors. Green Chemistry. 2007;9:654-62.

[9] Han C, Harrison DP. Simultaneous shift reaction and carbon dioxide separation for the direct production of hydrogen. Chemical Engineering Science. 1994;49:5875-83.

[10] Ochoa-Fernández E, Haugen G, Zhao T, Rønning M, Aartun I, Børresen B, et al. Process design simulation of H 2 production by sorption enhanced steam methane reforming: evaluation of potential CO 2 acceptors. Green Chemistry. 2007;9:654-62.

[11] Alvarez D, Abanades JC. Determination of the critical product layer thickness in the reaction of CaO with CO2. Industrial & engineering chemistry research. 2005;44:5608-15.

[12] Molinder RA. CO2 capture materials for sorption enhanced steam reforming: University of Leeds; 2012.

[13] Fernandez J, Abanades J, Murillo R. Modeling of sorption enhanced steam methane reforming in an adiabatic fixed bed reactor. Chemical Engineering Science. 2012;84:1-11.

[14] Lee DK, Baek IH, Yoon WL. Modeling and simulation for the methane steam reforming enhanced by in situ CO 2 removal utilizing the CaO carbonation for H 2 production. Chemical Engineering Science. 2004;59:931-42.

[15] Koumpouras GC, Alpay E, Stepanek F. Mathematical modelling of low-temperature hydrogen production with in situ CO$_2$ capture. Chemical Engineering Science. 2007;62:2833-41.

[16] Ding Y, Alpay E. Adsorption-enhanced steam–methane reforming. Chemical Engineering Science. 2000;55:3929-40.

[17] Xiu G, Li P, Rodrigues AE. Adsorption-enhanced steam-methane reforming with intraparticle-diffusion limitations. Chemical Engineering Journal. 2003;95:83-93.

[18] Li Z-s, Cai N-s. Modeling of multiple cycles for sorption-enhanced steam methane reforming and sorbent regeneration in fixed bed reactor. Energy & Fuels. 2007;21:2909-18.

[19] Baker E. 87. The calcium oxide–carbon dioxide system in the pressure range 1—300 atmospheres. Journal of the Chemical Society (Resumed). 1962:464-70.

[20] Bhatia S, Perlmutter D. Effect of the product layer on the kinetics of the CO2-lime reaction. AIChE Journal. 1983;29:79-86.

[21] Rodríguez N, Alonso M, Abanades J. Experimental investigation of a circulating fluidized-bed reactor to capture CO2 with CaO. AIChE Journal. 2011;57:1356-66.

[22] Dedman A, Owen A. Calcium cyanamide synthesis. Part 4.—The reaction CaO+ CO 2= CaCo 3. Transactions of the Faraday Society. 1962;58:2027-35.

[23] Rostrup-Nielsen JR. Catalytic steam reforming: Springer; 1984.

[24] Rostrup-Nielsen JR, Rostrup-Nielsen T. Large-scale hydrogen production. Cattech. 2002;6:150-9.

[25] Rydén M, Ramos P. H 2 production with CO 2 capture by sorption enhanced chemical-looping reforming using NiO as oxygen carrier and CaO as CO 2 sorbent. Fuel Processing Technology. 2012;96:27-36.

[26] Meyer J, Mastin J, Bjørnebøle T-K, Ryberg T, Eldrup N. Techno-economical study of the Zero Emission Gas power concept. Energy Procedia. 2011;4:1949-56.

[27] Stevens JF, Krishnamurthy B, Atanassova P, Spilker K. Development of 50 kW fuel processor for stationary fuel cell applications. Chevron Techology Ventures, LLC; 2007.

[28] Fernandez J, Abanades J, Grasa G. Modeling of Sorption Enhanced Steam Methane Reforming. Part II: Simulation within a novel Ca/Cu chemical loop process for hydrogen production. Chemical Engineering Science. 2012.

[29] Rostrup-Nielsen J, Sehested J, Nørskov JK. Hydrogen and synthesis gas by steam-and CO 2 reforming. Advances in Catalysis2002.

[30] Edwards M, Richardson J. Gas dispersion in packed beds. Chemical Engineering Science. 1968;23:109-23.

[31] Yagi S, Kunii D, Wakao N. Studies on axial effective thermal conductivities in packed beds. AIChE Journal. 1960;6:543-6.

[32] Geankoplis CJ. Transport processes and unit operations. 1993.

[33] Handley D, Heggs PJ. The effect of thermal conductivity of the packing material on transient heat transfer in a fixed bed. International Journal of Heat and Mass Transfer. 1969;12:549-70.